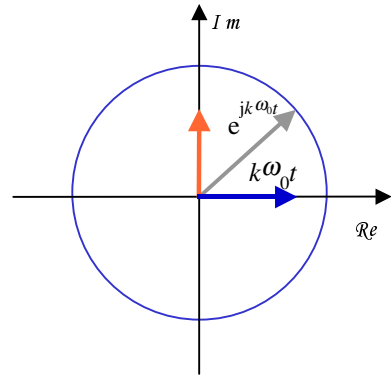


9



POWER SPECTRUM AND CORRELATION

- 9.1 Power Spectrum and Correlation
- 9.2 Fourier Series: Representation of Periodic Signals
- 9.3 Fourier Transform: Representation of Aperiodic Signals
- 9.4 Non-Parametric Power Spectral Estimation
- 9.5 Model-Based Power Spectral Estimation
- 9.6 High Resolution Spectral Estimation Based on Subspace Eigen-Analysis
- 9.7 Summary

The power spectrum reveals the existence, or the absence, of repetitive patterns and correlation structures in a signal process. These structural patterns are important in a wide range of applications such as data forecasting, signal coding, signal detection, radar, pattern recognition, and decision-making systems. The most common method of spectral estimation is based on the fast Fourier transform (FFT). For many applications, FFT-based methods produce sufficiently good results. However, more advanced methods of spectral estimation can offer better frequency resolution, and less variance. This chapter begins with an introduction to the Fourier series and transform and the basic principles of spectral estimation. The classical methods for power spectrum estimation are based on periodograms. Various methods of averaging periodograms, and their effects on the variance of spectral estimates, are considered. We then study the maximum entropy and the model-based spectral estimation methods. We also consider several high-resolution spectral estimation methods, based on eigen-analysis, for the estimation of sinusoids observed in additive white noise.

9.1 Power Spectrum and Correlation

The power spectrum of a signal gives the distribution of the signal power among various frequencies. The power spectrum is the Fourier transform of the correlation function, and reveals information on the correlation structure of the signal. The strength of the Fourier transform in signal analysis and pattern recognition is its ability to reveal spectral structures that may be used to characterise a signal. This is illustrated in Figure 9.1 for the two extreme cases of a sine wave and a purely random signal. For a periodic signal, the power is concentrated in extremely narrow bands of frequencies, indicating the existence of structure and the predictable character of the signal. In the case of a pure sine wave as shown in Figure 9.1(a) the signal power is concentrated in one frequency. For a purely random signal as shown in Figure 9.1(b) the signal power is spread equally in the frequency domain, indicating the lack of structure in the signal.

In general, the more correlated or predictable a signal, the more concentrated its power spectrum, and conversely the more random or unpredictable a signal, the more spread its power spectrum. Therefore the power spectrum of a signal can be used to deduce the existence of repetitive structures or correlated patterns in the signal process. Such information is crucial in detection, decision making and estimation problems, and in systems analysis.

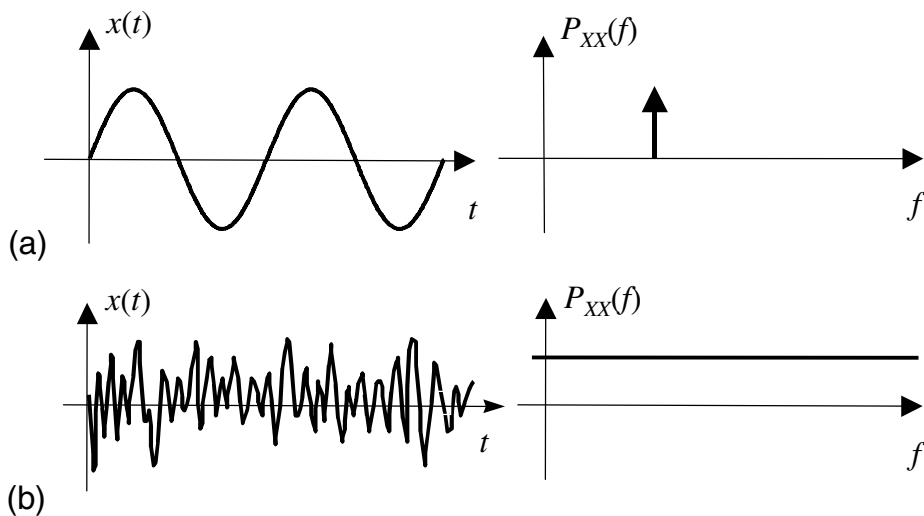


Figure 9.1 The concentration/spread of power in frequency indicates the correlated or random character of a signal: (a) a predictable signal, (b) a random signal.

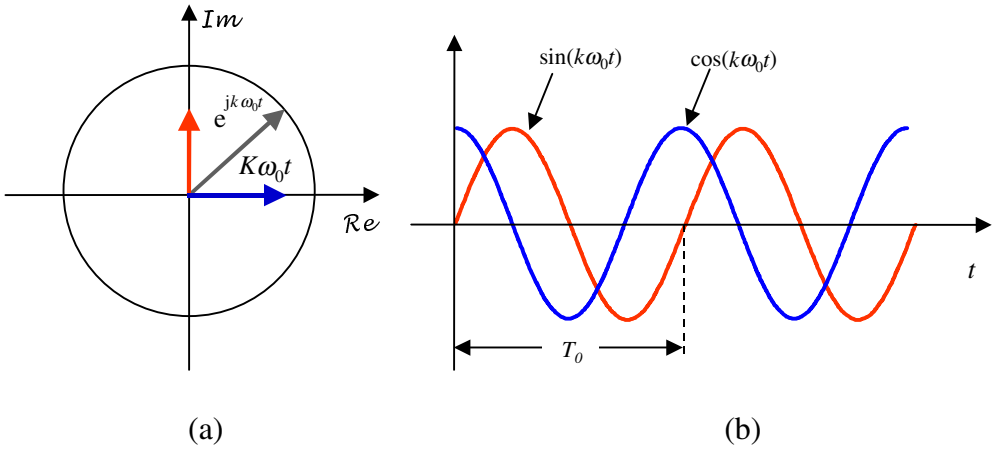


Figure 9.2 Fourier basis functions: (a) real and imaginary parts of a complex sinusoid, (b) vector representation of a complex exponential.

9.2 Fourier Series: Representation of Periodic Signals

The following three sinusoidal functions form the *basis functions* for the Fourier analysis:

$$x_1(t) = \cos \omega_0 t \tag{9.1}$$

$$x_2(t) = \sin \omega_0 t \tag{9.2}$$

$$x_3(t) = \cos \omega_0 t + j \sin \omega_0 t = e^{j\omega_0 t} \tag{9.3}$$

Figure 9.2(a) shows the cosine and the sine components of the complex exponential (cisoidal) signal of Equation (9.3), and Figure 9.2(b) shows a vector representation of the complex exponential in a complex plane with real (Re) and imaginary (Im) dimensions. The Fourier basis functions are periodic with an angular frequency of ω_0 (rad/s) and a period of $T_0 = 2\pi/\omega_0 = 1/F_0$, where F_0 is the frequency (Hz). The following properties make the sinusoids the ideal choice as the elementary building block basis functions for signal analysis and synthesis:

- (i) Orthogonality: two sinusoidal functions of *different* frequencies have the following orthogonal property:

$$\int_{-\infty}^{\infty} \sin(\omega_1 t) \sin(\omega_2 t) dt = \frac{1}{2} \int_{-\infty}^{\infty} \cos(\omega_1 + \omega_2) dt + \frac{1}{2} \int_{-\infty}^{\infty} \cos(\omega_1 - \omega_2) dt = 0 \quad (9.4)$$

For harmonically related sinusoids, the integration can be taken over one period. Similar equations can be derived for the product of cosines, or sine and cosine, of different frequencies. Orthogonality implies that the sinusoidal basis functions are independent and can be processed independently. For example, in a graphic equaliser, we can change the relative amplitudes of one set of frequencies, such as the bass, without affecting other frequencies, and in sub-band coding different frequency bands are coded independently and allocated different numbers of bits.

- (ii) Sinusoidal functions are infinitely differentiable. This is important, as most signal analysis, synthesis and manipulation methods require the signals to be differentiable.
- (iii) Sine and cosine signals of the same frequency have only a phase difference of $\pi/2$ or equivalently a relative time delay of a quarter of one period i.e. $T_0/4$.

Associated with the complex exponential function $e^{j\omega_0 t}$ is a set of harmonically related complex exponentials of the form

$$[1, e^{\pm j\omega_0 t}, e^{\pm j2\omega_0 t}, e^{\pm j3\omega_0 t}, \dots] \quad (9.5)$$

The set of exponential signals in Equation (9.5) are periodic with a fundamental frequency $\omega_0 = 2\pi/T_0 = 2\pi F_0$, where T_0 is the period and F_0 is the fundamental frequency. These signals form the set of *basis functions* for the Fourier analysis. Any linear combination of these signals of the form

$$\sum_{k=-\infty}^{\infty} c_k e^{jk\omega_0 t} \quad (9.6)$$

is also periodic with a period T_0 . Conversely any periodic signal $x(t)$ can be synthesised from a linear combination of harmonically related exponentials. The Fourier series representation of a periodic signal is given by the following synthesis and analysis equations:

$$x(t) = \sum_{k=-\infty}^{\infty} c_k e^{jk\omega_0 t} \quad k = \dots -1, 0, 1, \dots \quad (\text{synthesis equation}) \quad (9.7)$$

$$c_k = \frac{1}{T_0} \int_{-T_0/2}^{T_0/2} x(t) e^{-jk\omega_0 t} dt \quad k = \dots -1, 0, 1, \dots \quad (\text{analysis equation}) \quad (9.8)$$

The complex-valued coefficient c_k conveys the amplitude (a measure of the strength) and the phase of the frequency content of the signal at $k\omega_0$ (Hz). Note from Equation (9.8) that the coefficient c_k *may be interpreted as a measure of the correlation of the signal $x(t)$ and the complex exponential $e^{-jk\omega_0 t}$.*

9.3 Fourier Transform: Representation of Aperiodic Signals

The Fourier series representation of periodic signals consist of harmonically related spectral lines spaced at integer multiples of the fundamental frequency. The Fourier representation of aperiodic signals can be developed by regarding an aperiodic signal as a special case of a periodic signal with an infinite period. If the period of a signal is infinite then the signal does not repeat itself, and is aperiodic.

Now consider the discrete spectra of a periodic signal with a period of T_0 , as shown in Figure 9.3(a). As the period T_0 is increased, the fundamental frequency $F_0=1/T_0$ decreases, and successive spectral lines become more closely spaced. In the limit as the period tends to infinity (i.e. as the signal becomes aperiodic), the discrete spectral lines merge and form a continuous spectrum. Therefore the Fourier equations for an aperiodic signal (known as the Fourier transform) must reflect the fact that the frequency spectrum of an aperiodic signal is continuous. Hence, to obtain the Fourier transform relation, the discrete-frequency variables and operations in the Fourier series Equations (9.7) and (9.8) should be replaced by their continuous-frequency counterparts. That is, the discrete summation sign Σ should be replaced by the continuous summation integral \int , the discrete harmonics of the fundamental frequency kF_0 should be replaced by the continuous frequency variable f , and the discrete frequency spectrum c_k should be replaced by a continuous frequency spectrum say $X(f)$.

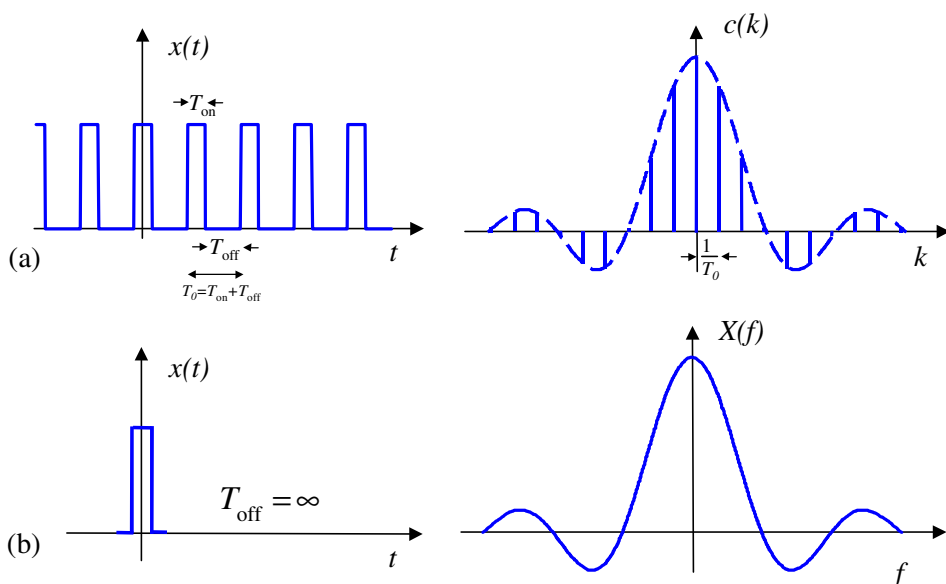


Figure 9.3 (a) A periodic pulse train and its line spectrum. (b) A single pulse from the periodic train in (a) with an imagined “off” duration of infinity; its spectrum is the envelope of the spectrum of the periodic signal in (a).

The Fourier synthesis and analysis equations for aperiodic signals, the so-called *Fourier transform pair*, are given by

$$x(t) = \int_{-\infty}^{\infty} X(f) e^{j2\pi ft} df \quad (9.9)$$

$$X(f) = \int_{-\infty}^{\infty} x(t) e^{-j2\pi ft} dt \quad (9.10)$$

Note from Equation (9.10), that $X(f)$ may be interpreted as a measure of the correlation of the signal $x(t)$ and the complex sinusoid $e^{-j2\pi ft}$.

The condition for existence and computability of the Fourier transform integral of a signal $x(t)$ is that the signal must have finite energy:

$$\int_{-\infty}^{\infty} |x(t)|^2 dt < \infty \quad (9.11)$$

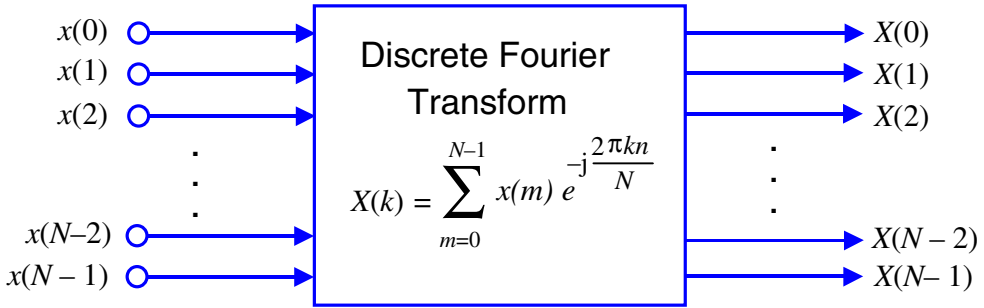


Figure 9.4 Illustration of the DFT as a parallel-input, parallel-output processor.

9.3.1 Discrete Fourier Transform (DFT)

For a finite-duration, discrete-time signal $x(m)$ of length N samples, the discrete Fourier transform (DFT) is defined as N uniformly spaced spectral samples

$$X(k) = \sum_{m=0}^{N-1} x(m) e^{-j(2\pi/N)mk}, \quad k = 0, \dots, N-1 \quad (9.12)$$

(see Figure9.4). The inverse discrete Fourier transform (IDFT) is given by

$$x(m) = \frac{1}{N} \sum_{k=0}^{N-1} X(k) e^{j(2\pi/N)mk}, \quad m = 0, \dots, N-1 \quad (9.13)$$

From Equation (9.13), the direct calculation of the Fourier transform requires $N(N-1)$ multiplications and a similar number of additions. Algorithms that reduce the computational complexity of the discrete Fourier transform are known as fast Fourier transforms (FFT) methods. FFT methods utilise the periodic and symmetric properties of $e^{-j2\pi/N}$ to avoid redundant calculations.

9.3.2 Time/Frequency Resolutions, The Uncertainty Principle

Signals such as speech, music or image are composed of non-stationary (i.e. time-varying and/or space-varying) events. For example, speech is composed of a string of short-duration sounds called phonemes, and an

image is composed of various objects. When using the DFT, it is desirable to have high enough time and space resolution in order to obtain the spectral characteristics of each individual elementary event or object in the input signal. However, there is a fundamental trade-off between the length, i.e. the time or space resolution, of the input signal and the frequency resolution of the output spectrum. The DFT takes as the input a window of N uniformly spaced time-domain samples $[x(0), x(1), \dots, x(N-1)]$ of duration $\Delta T = N \cdot T_s$, and outputs N spectral samples $[X(0), X(1), \dots, X(N-1)]$ spaced uniformly between zero Hz and the sampling frequency $F_s = 1/T_s$ Hz. Hence the frequency resolution of the DFT spectrum Δf , i.e. the space between successive frequency samples, is given by

$$\Delta f = \frac{1}{\Delta T} = \frac{1}{NT_s} = \frac{F_s}{N} \quad (9.14)$$

Note that the frequency resolution Δf and the time resolution ΔT are inversely proportional in that they cannot both be simultaneously increased; in fact, $\Delta T \Delta f = 1$. This is known as the uncertainty principle.

9.3.3 Energy-Spectral Density and Power-Spectral Density

Energy, or power, spectrum analysis is concerned with the distribution of the signal energy or power in the frequency domain. For a deterministic discrete-time signal, the energy-spectral density is defined as

$$|X(f)|^2 = \left| \sum_{m=-\infty}^{\infty} x(m) e^{-j2\pi f m} \right|^2 \quad (9.15)$$

The energy spectrum of $x(m)$ may be expressed as the Fourier transform of the autocorrelation function of $x(m)$:

$$\begin{aligned} |X(f)|^2 &= X(f) X^*(f) \\ &= \sum_{m=-\infty}^{\infty} r_{xx}(m) e^{-j2\pi f m} \end{aligned} \quad (9.16)$$

where the variable $r_{xx}(m)$ is the autocorrelation function of $x(m)$. The Fourier transform exists only for finite-energy signals. An important

theoretical class of signals is that of stationary stochastic signals, which, as a consequence of the stationarity condition, are infinitely long and have infinite energy, and therefore do not possess a Fourier transform. For stochastic signals, the quantity of interest is the power-spectral density, defined as the Fourier transform of the autocorrelation function:

$$P_{XX}(f) = \sum_{m=-\infty}^{\infty} r_{xx}(m) e^{-j2\pi fm} \quad (9.17)$$

where the autocorrelation function $r_{xx}(m)$ is defined as

$$r_{xx}(m) = \mathcal{E}[x(m)x(m+k)] \quad (9.18)$$

In practice, the autocorrelation function is estimated from a signal record of length N samples as

$$\hat{r}_{xx}(m) = \frac{1}{N-|m|} \sum_{k=0}^{N-|m|-1} x(k)x(k+m), \quad k=0, \dots, N-1 \quad (9.19)$$

In Equation (9.19), as the correlation lag m approaches the record length N , the estimate of $\hat{r}_{xx}(m)$ is obtained from the average of fewer samples and has a higher variance. A triangular window may be used to “down-weight” the correlation estimates for larger values of lag m . The triangular window has the form

$$w(m) = \begin{cases} 1 - \frac{|m|}{N}, & |m| \leq N-1 \\ 0, & \text{otherwise} \end{cases} \quad (9.20)$$

Multiplication of Equation (9.19) by the window of Equation (9.20) yields

$$\hat{r}_{xx}(m) = \frac{1}{N} \sum_{k=0}^{N-|m|-1} x(k)x(k+m) \quad (9.21)$$

The expectation of the windowed correlation estimate $\hat{r}_{xx}(m)$ is given by

$$\begin{aligned}\mathcal{E}[\hat{r}_{xx}(m)] &= \frac{1}{N} \sum_{k=0}^{N-|m|-1} \mathcal{E}[x(k)x(k+m)] \\ &= \left(1 - \frac{|m|}{N}\right) r_{xx}(m)\end{aligned}\tag{9.22}$$

In Jenkins and Watts, it is shown that the variance of $\hat{r}_{xx}(m)$ is given by

$$\text{Var}[\hat{r}_{xx}(m)] \approx \frac{1}{N} \sum_{k=-\infty}^{\infty} [r_{xx}^2(k) + r_{xx}(k-m)r_{xx}(k+m)]\tag{9.23}$$

From Equations (9.22) and (9.23), $\hat{r}_{xx}(m)$ is an asymptotically unbiased and consistent estimate.

9.4 Non-Parametric Power Spectrum Estimation

The classic method for estimation of the power spectral density of an N -sample record is the periodogram introduced by Sir Arthur Schuster in 1899. The periodogram is defined as

$$\begin{aligned}\hat{P}_{XX}(f) &= \frac{1}{N} \left| \sum_{m=0}^{N-1} x(m) e^{-j2\pi f m} \right|^2 \\ &= \frac{1}{N} |X(f)|^2\end{aligned}\tag{9.24}$$

The power-spectral density function, or power spectrum for short, defined in Equation (9.24), is the basis of non-parametric methods of spectral estimation. Owing to the finite length and the random nature of most signals, the spectra obtained from different records of a signal vary randomly about an average spectrum. A number of methods have been developed to reduce the variance of the periodogram.

9.4.1 The Mean and Variance of Periodograms

The mean of the periodogram is obtained by taking the expectation of Equation (9.24):

$$\begin{aligned}
\mathcal{E}[\hat{P}_{XX}(f)] &= \frac{1}{N} \mathcal{E} \left[|X(f)|^2 \right] \\
&= \frac{1}{N} \mathcal{E} \left[\sum_{m=0}^{N-1} x(m) e^{-j2\pi f m} \sum_{n=0}^{N-1} x(n) e^{j2\pi f n} \right] \\
&= \sum_{m=-(N-1)}^{N-1} \left(1 - \frac{|m|}{N} \right) r_{xx}(m) e^{-j2\pi f m}
\end{aligned} \tag{9.25}$$

As the number of signal samples N increases, we have

$$\lim_{N \rightarrow \infty} \mathcal{E}[\hat{P}_{XX}(f)] = \sum_{m=-\infty}^{\infty} r_{xx}(m) e^{-j2\pi f m} = P_{XX}(f) \tag{9.26}$$

For a Gaussian random sequence, the variance of the periodogram can be obtained as

$$\text{Var}[\hat{P}_{XX}(f)] = P_{XX}^2(f) \left[1 + \left(\frac{\sin 2\pi f N}{N \sin 2\pi f} \right)^2 \right] \tag{9.27}$$

As the length of a signal record N increases, the expectation of the periodogram converges to the power spectrum $P_{XX}(f)$ and the variance of $\hat{P}_{XX}(f)$ converges to $P_{XX}^2(f)$. Hence the periodogram is an unbiased but not a consistent estimate. The periodograms can be calculated from a DFT of the signal $x(m)$, or from a DFT of the autocorrelation estimates $\hat{r}_{xx}(m)$. In addition, the signal from which the periodogram, or the autocorrelation samples, are obtained can be segmented into overlapping blocks to result in a larger number of periodograms, which can then be averaged. These methods and their effects on the variance of periodograms are considered in the following.

9.4.2 Averaging Periodograms (Bartlett Method)

In this method, several periodograms, from different segments of a signal, are averaged in order to reduce the variance of the periodogram. The Bartlett periodogram is obtained as the average of K periodograms as

$$\hat{P}_{XX}^B(f) = \frac{1}{K} \sum_{i=1}^K \hat{P}_{XX}^{(i)}(f) \quad (9.28)$$

where $\hat{P}_{XX}^{(i)}(f)$ is the periodogram of the i^{th} segment of the signal. The expectation of the Bartlett periodogram $\hat{P}_{XX}^B(f)$ is given by

$$\begin{aligned} \mathcal{E}[\hat{P}_{XX}^B(f)] &= \mathcal{E}[\hat{P}_{XX}^{(i)}(f)] \\ &= \sum_{m=-(N-1)}^{N-1} \left(1 - \frac{|m|}{N}\right) r_{xx}(m) e^{-j2\pi f m} \\ &= \frac{1}{N} \int_{-1/2}^{1/2} P_{XX}(v) \left[\frac{\sin \pi(f-v)N}{\sin \pi(f-v)} \right]^2 dv \end{aligned} \quad (9.29)$$

where $(\sin \pi f N / \sin \pi f)^2 / N$ is the frequency response of the triangular window $1 - |m|/N$. From Equation (9.29), the Bartlett periodogram is asymptotically unbiased. The variance of $\hat{P}_{XX}^B(f)$ is $1/K$ of the variance of the periodogram, and is given by

$$\text{Var}[\hat{P}_{XX}^B(f)] = \frac{1}{K} P_{XX}^2(f) \left[1 + \left(\frac{\sin 2\pi f N}{N \sin 2\pi f} \right)^2 \right] \quad (9.30)$$

9.4.3 Welch Method: Averaging Periodograms from Overlapped and Windowed Segments

In this method, a signal $x(m)$, of length M samples, is divided into K overlapping segments of length N , and each segment is windowed prior to computing the periodogram. The i^{th} segment is defined as

$$x_i(m) = x(m + iD), \quad m=0, \dots, N-1, i=0, \dots, K-1 \quad (9.31)$$

where D is the overlap. For half-overlap $D=N/2$, while $D=N$ corresponds to no overlap. For the i^{th} windowed segment, the periodogram is given by

$$\hat{P}_{XX}^{(i)}(f) = \frac{1}{NU} \left| \sum_{m=0}^{N-1} w(m)x_i(m)e^{-j2\pi f m} \right|^2 \tag{9.32}$$

where $w(m)$ is the window function and U is the power in the window function, given by

$$U = \frac{1}{N} \sum_{m=0}^{N-1} w^2(m) \tag{9.33}$$

The spectrum of a finite-length signal typically exhibits side-lobes due to discontinuities at the endpoints. The window function $w(m)$ alleviates the discontinuities and reduces the spread of the spectral energy into the side-lobes of the spectrum. The Welch power spectrum is the average of K periodograms obtained from overlapped and windowed segments of a signal:

$$\hat{P}_{XX}^W(f) = \frac{1}{K} \sum_{i=0}^{K-1} \hat{P}_{XX}^{(i)}(f) \tag{9.34}$$

Using Equations (9.32) and (9.34), the expectation of $\hat{P}_{XX}^W(f)$ can be obtained as

$$\begin{aligned} \mathcal{E}[P_{XX}^W(f)] &= \mathcal{E}[\hat{P}_{XX}^{(i)}(f)] \\ &= \frac{1}{NU} \sum_{n=0}^{N-1} \sum_{m=0}^{N-1} w(n)w(m)\mathcal{E}[x_i(n)x_i(m)]e^{-j2\pi f(n-m)} \\ &= \frac{1}{NU} \sum_{n=0}^{N-1} \sum_{m=0}^{N-1} w(n)w(m)r_{xx}(n-m)e^{-j2\pi f(n-m)} \\ &= \int_{-1/2}^{1/2} P_{XX}(v)W(v-f)dv \end{aligned} \tag{9.35}$$

where

$$W(f) = \frac{1}{NU} \left| \sum_{m=0}^{N-1} w(m)e^{-j2\pi f m} \right|^2 \tag{9.36}$$

and the variance of the Welch estimate is given by

$$\text{Var}[\hat{P}_{XX}^W(f)] = \frac{1}{K^2} \sum_{i=0}^{K-1} \sum_{j=0}^{K-1} \mathcal{E} [\hat{P}_{XX}^{(i)}(f) \hat{P}_{XX}^{(j)}(f)] - (\mathcal{E}[\hat{P}_{XX}^W(f)])^2 \quad (9.37)$$

Welch has shown that for the case when there is no overlap, $D=N$,

$$\text{Var}[P_{XX}^W(f)] = \frac{\text{Var}[P_{XX}^{(i)}(f)]}{K_1} \approx \frac{P_{XX}^2(f)}{K_1} \quad (9.38)$$

and for half-overlap, $D=N/2$,

$$\text{Var}[\hat{P}_{XX}^W(f)] = \frac{9}{8K_2} P_{XX}^2(f) \quad (9.39)$$

9.4.4 Blackman–Tukey Method

In this method, an estimate of a signal power spectrum is obtained from the Fourier transform of the windowed estimate of the autocorrelation function as

$$\hat{P}_{XX}^{BT}(f) = \sum_{m=-(N-1)}^{N-1} w(m) \hat{r}_{xx}(m) e^{-j2\pi f m} \quad (9.40)$$

For a signal of N samples, the number of samples available for estimation of the autocorrelation value at the lag m , $\hat{r}_{xx}(m)$, decrease as m approaches N . Therefore, for large m , the variance of the autocorrelation estimate increases, and the estimate becomes less reliable. The window $w(m)$ has the effect of down-weighting the high variance coefficients at and around the end-points. The mean of the Blackman–Tukey power spectrum estimate is

$$\mathcal{E}[\hat{P}_{XX}^{BT}(f)] = \sum_{m=-(N-1)}^{N-1} \mathcal{E}[\hat{r}_{xx}(m)] w(m) e^{-j2\pi f m} \quad (9.41)$$

Now $\mathcal{E}[\hat{r}_{xx}(m)] = r_{xx}(m) w_B(m)$, where $w_B(m)$ is the Bartlett, or triangular, window. Equation (9.41) may be written as

$$\mathcal{E}[\hat{P}_{XX}^{BT}(f)] = \sum_{m=-(N-1)}^{N-1} r_{xx}(m)w_c(m)e^{-j2\pi fm} \tag{9.42}$$

where $w_c(m) = w_B(m)w(m)$. The right-hand side of Equation (9.42) can be written in terms of the Fourier transform of the autocorrelation and the window functions as

$$\mathcal{E}[\hat{P}_{XX}^{BT}(f)] = \int_{-1/2}^{1/2} P_{XX}(v)W_c(f-v)dv \tag{9.43}$$

where $W_c(f)$ is the Fourier transform of $w_c(m)$. The variance of the Blackman–Tukey estimate is given by

$$\text{Var}[\hat{P}_{XX}^{BT}(f)] \approx \frac{U}{N} P_{XX}^2(f) \tag{9.44}$$

where U is the energy of the window $w_c(m)$.

9.4.5 Power Spectrum Estimation from Autocorrelation of Overlapped Segments

In the Blackman–Tukey method, in calculating a correlation sequence of length N from a signal record of length N , progressively fewer samples are admitted in estimation of $\hat{r}_{xx}(m)$ as the lag m approaches the signal length N . Hence the variance of $\hat{r}_{xx}(m)$ increases with the lag m . This problem can be solved by using a signal of length $2N$ samples for calculation of N correlation values. In a generalisation of this method, the signal record $x(m)$, of length M samples, is divided into a number K of overlapping segments of length $2N$. The i^{th} segment is defined as

$$x_i(m) = x(m+iD), \quad m = 0, 1, \dots, 2N-1 \tag{9.45}$$

$$i = 0, 1, \dots, K-1$$

where D is the overlap. For each segment of length $2N$, the correlation function in the range of $0 \leq m \leq N$ is given by

$$\hat{r}_{xx}(m) = \frac{1}{N} \sum_{k=0}^{N-1} x_i(k)x_i(k+m), \quad m = 0, 1, \dots, N-1 \tag{9.46}$$

In Equation (9.46), the estimate of each correlation value is obtained as the averaged sum of N products.

9.5 Model-Based Power Spectrum Estimation

In non-parametric power spectrum estimation, the autocorrelation function is assumed to be zero for lags $|m| \geq N$, beyond which no estimates are available. In parametric or model-based methods, a model of the signal process is used to extrapolate the autocorrelation function beyond the range $|m| \leq N$ for which data is available. Model-based spectral estimators have a better resolution than the periodograms, mainly because they do not assume that the correlation sequence is zero-valued for the range of lags for which no measurements are available.

In linear model-based spectral estimation, it is assumed that the signal $x(m)$ can be modelled as the output of a linear time-invariant system excited with a random, flat-spectrum, excitation. The assumption that the input has a flat spectrum implies that the power spectrum of the model output is *shaped* entirely by the frequency response of the model. The input-output relation of a generalised discrete linear time-invariant model is given by

$$x(m) = \sum_{k=1}^P a_k x(m-k) + \sum_{k=0}^Q b_k e(m-k) \quad (9.47)$$

where $x(m)$ is the model output, $e(m)$ is the input, and the a_k and b_k are the parameters of the model. Equation (9.47) is known as an auto-regressive-moving-average (ARMA) model. The system function $H(z)$ of the discrete linear time-invariant model of Equation (9.47) is given by

$$H(z) = \frac{B(z)}{A(z)} = \frac{\sum_{k=0}^Q b_k z^{-k}}{1 - \sum_{k=1}^P a_k z^{-k}} \quad (9.48)$$

where $1/A(z)$ and $B(z)$ are the autoregressive and moving-average parts of $H(z)$ respectively. The power spectrum of the signal $x(m)$ is given as the product of the power spectrum of the input signal and the squared magnitude frequency response of the model:

$$P_{XX}(f) = P_{EE}(f) |H(f)|^2 \quad (9.49)$$

where $H(f)$ is the frequency response of the model and $P_{EE}(f)$ is the input power spectrum. Assuming that the input is a white noise process with unit variance, i.e. $P_{EE}(f)=1$, Equation (9.49) becomes

$$P_{XX}(f) = |H(f)|^2 \quad (9.50)$$

Thus the power spectrum of the model output is the squared magnitude of the frequency response of the model. An important aspect of model-based spectral estimation is the choice of the model. The model may be an auto regressive (all-pole), a moving-average (all-zero) or an ARMA (pole-zero) model.

9.5.1 Maximum-Entropy Spectral Estimation

The power spectrum of a stationary signal is defined as the Fourier transform of the autocorrelation sequence:

$$P_{XX}(f) = \sum_{n=-\infty}^{\infty} r_{xx}(m) e^{-j2\pi fm} \quad (9.51)$$

Equation (9.51) requires the autocorrelation $r_{xx}(m)$ for the lag m in the range $\pm\infty$. In practice, an estimate of the autocorrelation $r_{xx}(m)$ is available only for the values of m in a finite range of say $\pm P$. In general, there are an infinite number of different correlation sequences that have the same values in the range $|m| \leq P$ as the measured values. The particular estimate used in the non-parametric methods assumes the correlation values are zero for the lags beyond $\pm P$, for which no estimates are available. This arbitrary assumption results in spectral leakage and loss of frequency resolution. *The maximum-entropy estimate is based on the principle that the estimate of the autocorrelation sequence must correspond to the most random signal whose correlation values in the range $|m| \leq P$ coincide with the measured values.* The maximum-entropy principle is appealing because it assumes no more structure in the correlation sequence than that indicated by the measured data. The randomness or entropy of a signal is defined as

$$H[P_{XX}(f)] = \int_{-1/2}^{1/2} \ln P_{XX}(f) df \quad (9.52)$$

To obtain the maximum-entropy correlation estimate, we differentiate Equation (9.53) with respect to the unknown values of the correlation coefficients, and set the derivative to zero:

$$\frac{\partial H[P_{XX}(f)]}{\partial r_{xx}(m)} = \int_{-1/2}^{1/2} \frac{\partial \ln P_{XX}(f)}{\partial r_{xx}(m)} df = 0 \quad \text{for } |m| > P \quad (9.53)$$

Now, from Equation (9.17), the derivative of the power spectrum with respect to the autocorrelation values is given by

$$\frac{\partial P_{XX}(f)}{\partial r_{xx}(m)} = e^{-j2\pi fm} \quad (9.54)$$

From Equation (9.51), for the derivative of the logarithm of the power spectrum, we have

$$\frac{\partial \ln P_{XX}(f)}{\partial r_{xx}(m)} = P_{XX}^{-1}(f) e^{-j2\pi fm} \quad (9.55)$$

Substitution of Equation (9.55) in Equation (9.53) gives

$$\int_{-1/2}^{1/2} P_{XX}^{-1}(f) e^{-j2\pi fm} df = 0 \quad \text{for } |m| > P \quad (9.56)$$

Assuming that $P_{XX}^{-1}(f)$ is integrable, it may be associated with an autocorrelation sequence $c(m)$ as

$$P_{XX}^{-1}(f) = \sum_{m=-\infty}^{\infty} c(m) e^{-j2\pi fm} \quad (9.57)$$

where

$$c(m) = \int_{-1/2}^{1/2} P_{XX}^{-1}(f) e^{j2\pi fm} df \quad (9.58)$$

From Equations (9.56) and (9.58), we have $c(m)=0$ for $|m| > P$. Hence, from Equation (9.57), the inverse of the maximum-entropy power spectrum may be obtained from the Fourier transform of a finite-length autocorrelation sequence as

$$P_{XX}^{-1}(f) = \sum_{m=-P}^P c(m) e^{-j2\pi fm} \quad (9.59)$$

and the maximum-entropy power spectrum is given by

$$\hat{P}_{XX}^{ME}(f) = \frac{1}{\sum_{m=-P}^P c(m) e^{-j2\pi fm}} \quad (9.60)$$

Since the denominator polynomial in Equation (9.60) is symmetric, it follows that for every zero of this polynomial situated at a radius r , there is a zero at radius $1/r$. Hence this symmetric polynomial can be factorised and expressed as

$$\sum_{m=-P}^P c(m) z^{-m} = \frac{1}{\sigma^2} A(z) A(z^{-1}) \quad (9.61)$$

where $1/\sigma^2$ is a gain term, and $A(z)$ is a polynomial of order P defined as

$$A(z) = 1 + a_1 z^{-1} + \dots + a_p z^{-P} \quad (9.62)$$

From Equations (9.60) and (9.61), the maximum-entropy power spectrum may be expressed as

$$\hat{P}_{XX}^{ME}(f) = \frac{\sigma^2}{A(z) A(z^{-1})} \quad (9.63)$$

Equation (9.63) shows that the maximum-entropy power spectrum estimate is the power spectrum of an autoregressive (AR) model. Equation (9.63) was obtained by maximising the entropy of the power spectrum with respect to the unknown autocorrelation values. The known values of the autocorrelation function can be used to obtain the coefficients of the AR model of Equation (9.63), as discussed in the next section.

9.5.2 Autoregressive Power Spectrum Estimation

In the preceding section, it was shown that the maximum-entropy spectrum is equivalent to the spectrum of an autoregressive model of the signal. An autoregressive, or linear prediction model, described in detail in Chapter 8, is defined as

$$x(m) = \sum_{k=1}^P a_k x(m-k) + e(m) \quad (9.64)$$

where $e(m)$ is a random signal of variance σ_e^2 . The power spectrum of an autoregressive process is given by

$$P_{XX}^{AR}(f) = \frac{\sigma_e^2}{\left| 1 - \sum_{k=1}^P a_k e^{-j2\pi f k} \right|^2} \quad (9.65)$$

An AR model extrapolates the correlation sequence beyond the range for which estimates are available. The relation between the autocorrelation values and the AR model parameters is obtained by multiplying both sides of Equation (9.64) by $x(m-j)$ and taking the expectation:

$$\mathcal{E}[x(m)x(m-j)] = \sum_{k=1}^P a_k \mathcal{E}[x(m-k)x(m-j)] + \mathcal{E}[e(m)x(m-j)] \quad (9.66)$$

Now for the optimal model coefficients the random input $e(m)$ is orthogonal to the past samples, and Equation (9.66) becomes

$$r_{xx}(j) = \sum_{k=1}^P a_k r_{xx}(j-k), \quad j=1, 2, \dots \quad (9.67)$$

Given $P+1$ correlation values, Equation (9.67) can be solved to obtain the AR coefficients a_k . Equation (9.67) can also be used to extrapolate the correlation sequence. The methods of solving the AR model coefficients are discussed in Chapter 8.

9.5.3 Moving-Average Power Spectrum Estimation

A moving-average model is also known as an all-zero or a finite impulse response (FIR) filter. A signal $x(m)$, modelled as a moving-average process, is described as

$$x(m) = \sum_{k=0}^Q b_k e(m-k) \quad (9.68)$$

where $e(m)$ is a zero-mean random input and Q is the model order. The cross-correlation of the input and output of a moving average process is given by

$$\begin{aligned} r_{xe}(m) &= \mathcal{E}[x(j)e(j-m)] \\ &= \mathcal{E}\left[\sum_{k=0}^Q b_k e(j-k)e(j-m)\right] = \sigma_e^2 b_m \end{aligned} \quad (9.69)$$

and the autocorrelation function of a moving average process is

$$r_{xx}(m) = \begin{cases} \sigma_e^2 \sum_{k=0}^{Q-|m|} b_k b_{k+m}, & |m| \leq Q \\ 0, & |m| > Q \end{cases} \quad (9.70)$$

From Equation (9.70), the power spectrum obtained from the Fourier transform of the autocorrelation sequence is the same as the power spectrum of a moving average model of the signal. Hence the power spectrum of a moving-average process may be obtained directly from the Fourier transform of the autocorrelation function as

$$P_{XX}^{MA} = \sum_{m=-Q}^Q r_{xx}(m) e^{-j2\pi fm} \quad (9.71)$$

Note that the moving-average spectral estimation is identical to the Blackman–Tukey method of estimating periodograms from the autocorrelation sequence.

9.5.4 Autoregressive Moving-Average Power Spectrum Estimation

The ARMA, or pole-zero, model is described by Equation (9.47). The relationship between the ARMA parameters and the autocorrelation sequence can be obtained by multiplying both sides of Equation (9.47) by $x(m-j)$ and taking the expectation:

$$r_{xx}(j) = -\sum_{k=1}^P a_k r_{xx}(j-k) + \sum_{k=0}^Q b_k r_{xe}(j-k) \quad (9.72)$$

The moving-average part of Equation (9.72) influences the autocorrelation values only up to the lag of Q . Hence, for the autoregressive part of Equation (9.72), we have

$$r_{xx}(m) = -\sum_{k=1}^P a_k r_{xx}(m-k) \quad \text{for } m > Q \quad (9.73)$$

Hence Equation (9.73) can be used to obtain the coefficients a_k , which may then be substituted in Equation (9.72) for solving the coefficients b_k . Once the coefficients of an ARMA model are identified, the spectral estimate is given by

$$P_{XX}^{ARMA}(f) = \sigma_e^2 \frac{\left| \sum_{k=0}^Q b_k e^{-j2\pi f k} \right|^2}{\left| 1 + \sum_{k=1}^P a_k e^{-j2\pi f k} \right|^2} \quad (9.74)$$

where σ_e^2 is the variance of the input of the ARMA model. In general, the poles model the resonances of the signal spectrum, whereas the zeros model the anti-resonances of the spectrum.

9.6 High-Resolution Spectral Estimation Based on Subspace Eigen-Analysis

The eigen-based methods considered in this section are primarily used for estimation of the parameters of sinusoidal signals observed in an additive white noise. Eigen-analysis is used for partitioning the eigenvectors and the

eigenvalues of the autocorrelation matrix of a noisy signal into two subspaces:

- (a) the signal subspace composed of the *principle* eigenvectors associated with the largest eigenvalues;
- (b) the noise subspace represented by the smallest eigenvalues.

The decomposition of a noisy signal into a signal subspace and a noise subspace forms the basis of the eigen-analysis methods considered in this section.

9.6.1 Pisarenko Harmonic Decomposition

A real-valued sine wave can be modelled by a second-order autoregressive (AR) model, with its poles on the unit circle at the angular frequency of the sinusoid as shown in Figure 9.5. The AR model for a sinusoid of frequency F_i at a sampling rate of F_s is given by

$$x(m) = 2\cos(2\pi F_i / F_s) x(m-1) - x(m-2) + A\delta(m-t_0) \tag{9.75}$$

where $A\delta(m-t_0)$ is the initial impulse for a sine wave of amplitude A . In general, a signal composed of P real sinusoids can be modelled by an AR model of order $2P$ as

$$x(m) = \sum_{k=1}^{2P} a_k x(m-k) + A\delta(m-t_0) \tag{9.76}$$

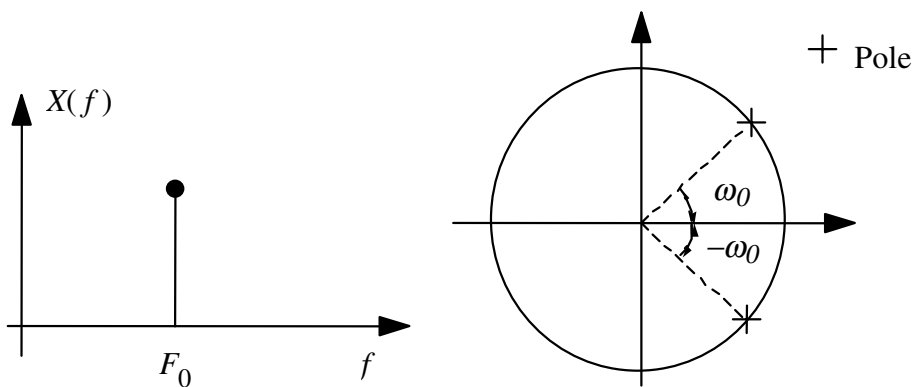


Figure 9.5 A second order all pole model of a sinusoidal signal.

The transfer function of the AR model is given by

$$H(z) = \frac{A}{1 - \sum_{k=1}^{2P} a_k z^{-k}} = \frac{A}{\prod_{k=1}^P (1 - e^{-j2\pi F_k} z^{-1})(1 - e^{+j2\pi F_k} z^{-1})} \quad (9.77)$$

where the angular positions of the poles on the unit circle, $e^{\pm j2\pi F_k}$, correspond to the angular frequencies of the sinusoids. For P real sinusoids observed in an additive white noise, we can write

$$\begin{aligned} y(m) &= x(m) + n(m) \\ &= \sum_{k=1}^{2P} a_k x(m-k) + n(m) \end{aligned} \quad (9.78)$$

Substituting $[y(m-k) - n(m-k)]$ for $x(m-k)$ in Equation (9.73) yields

$$y(m) - \sum_{k=1}^{2P} a_k y(m-k) = n(m) - \sum_{k=1}^{2P} a_k n(m-k) \quad (9.79)$$

From Equation (9.79), the noisy sinusoidal signal $y(m)$ can be modelled by an ARMA process in which the AR and the MA sections are identical, and the input is the noise process. Equation (9.79) can also be expressed in a vector notation as

$$\mathbf{y}^T \mathbf{a} = \mathbf{n}^T \mathbf{a} \quad (9.80)$$

where $\mathbf{y}^T = [y(m), \dots, y(m-2P)]$, $\mathbf{a}^T = [1, a_1, \dots, a_{2P}]$ and $\mathbf{n}^T = [n(m), \dots, n(m-2P)]$. To obtain the parameter vector \mathbf{a} , we multiply both sides of Equation (9.80) by the vector \mathbf{y} and take the expectation:

$$\mathcal{E}[\mathbf{y}\mathbf{y}^T] \mathbf{a} = \mathcal{E}[\mathbf{y}\mathbf{n}^T] \mathbf{a} \quad (9.81)$$

or

$$\mathbf{R}_{yy} \mathbf{a} = \mathbf{R}_{yn} \mathbf{a} \quad (9.82)$$

where $\mathcal{E}[\mathbf{y}\mathbf{y}^T] = \mathbf{R}_{yy}$, and $\mathcal{E}[\mathbf{y}\mathbf{n}^T] = \mathbf{R}_{yn}$ can be written as

$$\begin{aligned} \mathbf{R}_{yn} &= \mathcal{E}[(x+n)\mathbf{n}^T] \\ &= \mathcal{E}[\mathbf{nn}^T] = \mathbf{R}_{nn} = \sigma_n^2 \mathbf{I} \end{aligned} \quad (9.83)$$

where σ_n^2 is the noise variance. Using Equation (9.83), Equation (9.82) becomes

$$\mathbf{R}_{yy} \mathbf{a} = \sigma_n^2 \mathbf{a} \quad (9.84)$$

Equation (9.84) is in the form of an eigenequation. If the dimension of the matrix \mathbf{R}_{yy} is greater than $2P \times 2P$ then the largest $2P$ eigenvalues are associated with the eigenvectors of the noisy sinusoids and the minimum eigenvalue corresponds to the noise variance σ_n^2 . The parameter vector \mathbf{a} is obtained as the eigenvector of \mathbf{R}_{yy} , with its first element unity and associated with the minimum eigenvalue. From the AR parameter vector \mathbf{a} , we can obtain the frequencies of the sinusoids by first calculating the roots of the polynomial

$$1 + a_1 z^{-1} + a_2 z^{-2} + \dots + a_2 z^{-2P+2} + a_1 z^{-2P+1} + z^{-2P} = 0 \quad (9.85)$$

Note that for sinusoids, the AR parameters form a symmetric polynomial; that is $a_k = a_{2P-k}$. The frequencies F_k of the sinusoids can be obtained from the roots z_k of Equation (9.85) using the relation

$$z_k = e^{j2\pi F_k} \quad (9.86)$$

The powers of the sinusoids are calculated as follows. For P sinusoids observed in additive white noise, the autocorrelation function is given by

$$r_{yy}(k) = \sum_{i=1}^P P_i \cos 2k\pi F_i + \sigma_n^2 \delta(k) \quad (9.87)$$

where $P_i = A_i^2 / 2$ is the power of the sinusoid $A_i \sin(2\pi F_i)$, and white noise affects only the correlation at lag zero $r_{yy}(0)$. Hence Equation (9.87) for the correlation lags $k=1, \dots, P$ can be written as

$$\begin{pmatrix} \cos 2\pi F_1 & \cos 2\pi F_2 & \dots & \cos 2\pi F_P \\ \cos 4\pi F_1 & \cos 4\pi F_2 & \dots & \cos 4\pi F_P \\ \vdots & \vdots & \ddots & \vdots \\ \cos 2P\pi F_1 & \cos 2P\pi F_2 & \dots & \cos 2P\pi F_P \end{pmatrix} \begin{pmatrix} P_1 \\ P_2 \\ \vdots \\ P_P \end{pmatrix} = \begin{pmatrix} r_{yy}(1) \\ r_{yy}(2) \\ \vdots \\ r_{yy}(P) \end{pmatrix} \quad (9.88)$$

Given an estimate of the frequencies F_i from Equations (9.85) and (86), and an estimate of the autocorrelation function $\hat{r}_{yy}(k)$, Equation (9.88) can be solved to obtain the powers of the sinusoids P_i . The noise variance can then be obtained from Equation (9.87) as

$$\sigma_n^2 = r_{yy}(0) - \sum_{i=1}^P P_i \quad (9.89)$$

9.6.2 Multiple Signal Classification (MUSIC) Spectral Estimation

The MUSIC algorithm is an eigen-based subspace decomposition method for estimation of the frequencies of complex sinusoids observed in additive white noise. Consider a signal $y(m)$ modelled as

$$y(m) = \sum_{k=1}^P A_k e^{-j(2\pi F_k m + \phi_k)} + n(m) \quad (9.90)$$

An N -sample vector $\mathbf{y} = [y(m), \dots, y(m+N-1)]$ of the noisy signal can be written as

$$\begin{aligned} \mathbf{y} &= \mathbf{x} + \mathbf{n} \\ &= \mathbf{S}\mathbf{a} + \mathbf{n} \end{aligned} \quad (9.91)$$

where the signal vector $\mathbf{x} = \mathbf{S}\mathbf{a}$ is defined as

$$\begin{pmatrix} x(m) \\ x(m+1) \\ \vdots \\ x(m+N-1) \end{pmatrix} = \begin{pmatrix} e^{j2\pi F_1 m} & e^{j2\pi F_2 m} & \dots & e^{j2\pi F_P m} \\ e^{j2\pi F_1 (m+1)} & e^{j2\pi F_2 (m+1)} & \dots & e^{j2\pi F_P (m+1)} \\ \vdots & \vdots & \ddots & \vdots \\ e^{j2\pi F_1 (m+N-1)} & e^{j2\pi F_2 (m+N-1)} & \dots & e^{j2\pi F_P (m+N-1)} \end{pmatrix} \begin{pmatrix} A_1 e^{j2\pi \phi_1} \\ A_2 e^{j2\pi \phi_2} \\ \vdots \\ A_P e^{j2\pi \phi_P} \end{pmatrix} \quad (9.92)$$

The matrix \mathbf{S} and the vector \mathbf{a} are defined on the right-hand side of Equation (9.92). The autocorrelation matrix of the noisy signal \mathbf{y} can be written as the sum of the autocorrelation matrices of the signal \mathbf{x} and the noise as

$$\begin{aligned}\mathbf{R}_{yy} &= \mathbf{R}_{xx} + \mathbf{R}_{nn} \\ &= \mathbf{S}\mathbf{P}\mathbf{S}^H + \sigma_n^2\mathbf{I}\end{aligned}\quad (9.93)$$

where $\mathbf{R}_{xx} = \mathbf{S}\mathbf{P}\mathbf{S}^H$ and $\mathbf{R}_{nn} = \sigma_n^2\mathbf{I}$ are the autocorrelation matrices of the signal and noise processes, the exponent H denotes the Hermitian transpose, and the diagonal matrix \mathbf{P} defines the power of the sinusoids as

$$\mathbf{P} = \mathbf{a}\mathbf{a}^H = \text{diag}[P_1, P_2, \dots, P_P] \quad (9.94)$$

where $P_i = A_i^2$ is the power of the complex sinusoid $e^{-j2\pi F_i}$. The correlation matrix of the signal can also be expressed in the form

$$\mathbf{R}_{xx} = \sum_{k=1}^P P_k \mathbf{s}_k \mathbf{s}_k^H \quad (9.95)$$

where $\mathbf{s}_k^H = [1, e^{j2\pi F_k}, \dots, e^{j2\pi(N-1)F_k}]$. Now consider an eigen-decomposition of the $N \times N$ correlation matrix \mathbf{R}_{xx}

$$\begin{aligned}\mathbf{R}_{xx} &= \sum_{k=1}^N \lambda_k \mathbf{v}_k \mathbf{v}_k^H \\ &= \sum_{k=1}^P \lambda_k \mathbf{v}_k \mathbf{v}_k^H\end{aligned}\quad (9.96)$$

where λ_k and \mathbf{v}_k are the eigenvalues and eigenvectors of the matrix \mathbf{R}_{xx} respectively. We have also used the fact that the autocorrelation matrix \mathbf{R}_{xx} of P complex sinusoids has only P non-zero eigenvalues, $\lambda_{p+1} = \lambda_{p+2} = \dots = \lambda_N = 0$. Since the sum of the cross-products of the eigenvectors forms an identity matrix we can also express the diagonal autocorrelation matrix of the noise in terms of the eigenvectors of \mathbf{R}_{xx} as

$$\mathbf{R}_{nn} = \sigma_n^2 \mathbf{I} = \sigma_n^2 \sum_{k=1}^N \mathbf{v}_k \mathbf{v}_k^H \quad (9.97)$$

The correlation matrix of the noisy signal may be expressed in terms of its eigenvectors and the associated eigenvalues of the noisy signal as

$$\begin{aligned} \mathbf{R}_{yy} &= \sum_{k=1}^P \lambda_k \mathbf{v}_k \mathbf{v}_k^H + \sigma_n^2 \sum_{k=1}^N \mathbf{v}_k \mathbf{v}_k^H \\ &= \sum_{k=1}^P (\lambda_k + \sigma_n^2) \mathbf{v}_k \mathbf{v}_k^H + \sigma_n^2 \sum_{k=P+1}^N \mathbf{v}_k \mathbf{v}_k^H \end{aligned} \quad (9.98)$$

From Equation (9.98), the eigenvectors and the eigenvalues of the correlation matrix of the noisy signal can be partitioned into two disjoint subsets (see Figure 9.6). The set of eigenvectors $\{\mathbf{v}_1, \dots, \mathbf{v}_P\}$, associated with the P largest eigenvalues span the *signal subspace* and are called the *principal eigenvectors*. The signal vectors s_i can be expressed as linear combinations of the principal eigenvectors. The second subset of eigenvectors $\{\mathbf{v}_{P+1}, \dots, \mathbf{v}_N\}$ span the *noise subspace* and have σ_n^2 as their eigenvalues. Since the signal and noise eigenvectors are orthogonal, it follows that the signal subspace and the noise subspace are orthogonal. Hence the sinusoidal signal vectors s_i which are in the signal subspace, are orthogonal to the noise subspace, and we have

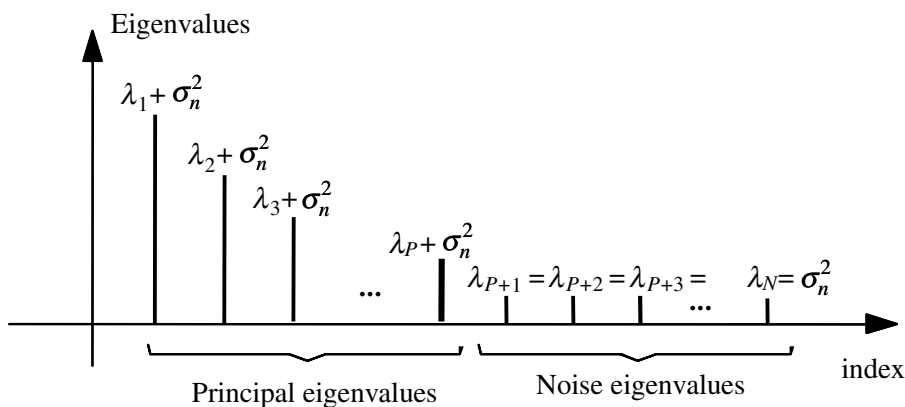


Figure 9.6 Decomposition of the eigenvalues of a noisy signal into the principal eigenvalues and the noise eigenvalues.

$$\mathbf{s}_i^H(f) \mathbf{v}_k = \sum_{m=0}^{N-1} v_k(m) e^{-j2\pi F_i m} = 0 \quad i = 1, \dots, P \quad k = P+1, \dots, N \quad (9.99)$$

Equation (9.99) implies that the frequencies of the P sinusoids can be obtained by solving for the zeros of the following polynomial function of the frequency variable f :

$$\sum_{k=P+1}^N \mathbf{s}^H(f) \mathbf{v}_k \quad (9.100)$$

In the MUSIC algorithm, the power spectrum estimate is defined as

$$P_{XX}(f) = \sum_{k=P+1}^N \left| \mathbf{s}^H(f) \mathbf{v}_k \right|^2 \quad (9.101)$$

where $\mathbf{s}(f) = [1, e^{j2\pi f}, \dots, e^{j2\pi(N-1)f}]$ is the complex sinusoidal vector, and $\{\mathbf{v}_{P+1}, \dots, \mathbf{v}_N\}$ are the eigenvectors in the noise subspace. From Equations (9.102) and (9.96) we have that

$$P_{XX}(f_i) = 0, \quad i = 1, \dots, P \quad (9.102)$$

Since $P_{XX}(f)$ has its zeros at the frequencies of the sinusoids, it follows that the reciprocal of $P_{XX}(f)$ has its poles at these frequencies. The MUSIC spectrum is defined as

$$P_{XX}^{MUSIC}(f) = \frac{1}{\sum_{k=P+1}^N \left| \mathbf{s}^H(f) \mathbf{v}_k \right|^2} = \frac{1}{\mathbf{s}^H(f) \mathbf{V}(f) \mathbf{V}^H(f) \mathbf{s}(f)} \quad (9.103)$$

where $\mathbf{V} = [\mathbf{v}_{P+1}, \dots, \mathbf{v}_N]$ is the matrix of eigenvectors of the noise subspace. $P_{MUSIC}(f)$ is sharply peaked at the frequencies of the sinusoidal components of the signal, and hence the frequencies of its peaks are taken as the MUSIC estimates.

9.6.3 Estimation of Signal Parameters via Rotational Invariance Techniques (ESPRIT)

The ESPRIT algorithm is an eigen-decomposition approach for estimating the frequencies of a number of complex sinusoids observed in additive white noise. Consider a signal $y(m)$ composed of P complex-valued sinusoids and additive white noise:

$$y(m) = \sum_{k=1}^P A_k e^{-j(2\pi F_k m + \phi_k)} + n(m) \quad (9.104)$$

The ESPRIT algorithm exploits the deterministic relation between sinusoidal component of the signal vector $\mathbf{y}(m) = [y(m), \dots, y(m+N-1)]^T$ and that of the time-shifted vector $\mathbf{y}(m+1) = [y(m+1), \dots, y(m+N)]^T$. The signal component of the noisy vector $\mathbf{y}(m)$ may be expressed as

$$\mathbf{x}(m) = \mathbf{S} \mathbf{a} \quad (9.105)$$

where \mathbf{S} is the complex sinusoidal matrix and \mathbf{a} is the vector containing the amplitude and phase of the sinusoids as in Equations (9.91) and (9.92). A complex sinusoid $e^{j2\pi F_i m}$ can be time-shifted by one sample through multiplication by a phase term $e^{j2\pi F_i}$. Hence the time-shifted sinusoidal signal vector $\mathbf{x}(m+1)$ may be obtained from $\mathbf{x}(m)$ by phase-shifting each complex sinusoidal component of $\mathbf{x}(m)$ as

$$\mathbf{x}(m+1) = \mathbf{S} \mathbf{\Phi} \mathbf{a} \quad (9.106)$$

where $\mathbf{\Phi}$ is a $P \times P$ phase matrix defined as

$$\mathbf{\Phi} = \text{diag}[e^{j2\pi F_1}, e^{j2\pi F_2}, \dots, e^{j2\pi F_P}] \quad (9.107)$$

The diagonal elements of $\mathbf{\Phi}$ are the relative phases between the adjacent samples of the sinusoids. The matrix $\mathbf{\Phi}$ is a unitary matrix and is known as a *rotation matrix* since it relates the time-shifted vectors $\mathbf{x}(m)$ and $\mathbf{x}(m+1)$. The autocorrelation matrix of the noisy signal vector $\mathbf{y}(m)$ can be written as

$$\mathbf{R}_{\mathbf{y}(m)\mathbf{y}(m)} = \mathbf{S} \mathbf{P} \mathbf{S}^H + \sigma_n^2 \mathbf{I} \quad (9.108)$$

where the matrix \mathbf{P} is diagonal, and its diagonal elements are the powers of the complex sinusoids $\mathbf{P} = \text{diag}[A_1^2, \dots, A_P^2] = \mathbf{a}\mathbf{a}^H$. The cross-covariance matrix of the vectors $\mathbf{y}(m)$ and $\mathbf{y}(m+1)$ is

$$\mathbf{R}_{\mathbf{y}(m)\mathbf{y}(m+1)} = \mathbf{S}\mathbf{P}\mathbf{\Phi}^H\mathbf{S}^H + \mathbf{R}_{\mathbf{n}(m)\mathbf{n}(m+1)} \quad (9.109)$$

where the autocovariance matrices $\mathbf{R}_{\mathbf{y}(m)\mathbf{y}(m+1)}$ and $\mathbf{R}_{\mathbf{n}(m)\mathbf{n}(m+1)}$ are defined as

$$\mathbf{R}_{\mathbf{y}(m)\mathbf{y}(m+1)} = \begin{pmatrix} r_{yy}(1) & r_{yy}(2) & r_{yy}(3) & \dots & r_{yy}(N) \\ r_{yy}(0) & r_{yy}(1) & r_{yy}(2) & \dots & r_{yy}(N-1) \\ r_{yy}(1) & r_{yy}(0) & r_{yy}(1) & \dots & r_{yy}(N-2) \\ \vdots & \vdots & \vdots & \ddots & \vdots \\ r_{yy}(N-2) & r_{yy}(N-3) & r_{yy}(N-4) & \dots & r_{yy}(1) \end{pmatrix} \quad (9.110)$$

and

$$\mathbf{R}_{\mathbf{n}(m)\mathbf{n}(m+1)} = \begin{pmatrix} 0 & 0 & \dots & 0 & 0 \\ \sigma_n^2 & 0 & \dots & 0 & 0 \\ 0 & \sigma_n^2 & \dots & 0 & 0 \\ \vdots & \vdots & \ddots & \vdots & \vdots \\ 0 & 0 & \dots & \sigma_n^2 & 0 \end{pmatrix} \quad (9.111)$$

The correlation matrix of the signal vector $\mathbf{x}(m)$ can be estimated as

$$\mathbf{R}_{\mathbf{x}(m)\mathbf{x}(m)} = \mathbf{R}_{\mathbf{y}(m)\mathbf{y}(m)} - \mathbf{R}_{\mathbf{n}(m)\mathbf{n}(m)} = \mathbf{S}\mathbf{P}\mathbf{S}^H \quad (9.112)$$

and the cross-correlation matrix of the signal vector $\mathbf{x}(m)$ with its time-shifted version $\mathbf{x}(m+1)$ is obtained as

$$\mathbf{R}_{\mathbf{x}(m)\mathbf{x}(m+1)} = \mathbf{R}_{\mathbf{y}(m)\mathbf{y}(m+1)} - \mathbf{R}_{\mathbf{n}(m)\mathbf{n}(m+1)} = \mathbf{S}\mathbf{P}\mathbf{\Phi}^H\mathbf{S}^H \quad (9.113)$$

Subtraction of a fraction $\lambda_i = e^{-j2\pi F_i}$ of Equation (9.113) from Equation (9.112) yields

$$\mathbf{R}_{\mathbf{x}(m)\mathbf{x}(m)} - \lambda_i \mathbf{R}_{\mathbf{x}(m)\mathbf{x}(m+1)} = \mathbf{S}\mathbf{P}(\mathbf{I} - \lambda_i \mathbf{\Phi}^H)\mathbf{S}^H \quad (9.114)$$

From Equations (9.107) and (9.114), the frequencies of the sinusoids can be estimated as the roots of Equation (9.114).

9.7 Summary

Power spectrum estimation is perhaps the most widely used method of signal analysis. The main objective of any transformation is to express a signal in a form that lends itself to more convenient analysis and manipulation. The power spectrum is related to the correlation function through the Fourier transform. The power spectrum reveals the repetitive and correlated patterns of a signal, which are important in detection, estimation, data forecasting and decision-making systems. We began this chapter with Section 9.1 on basic definitions of the Fourier series/transform, energy spectrum and power spectrum. In Section 9.2, we considered non-parametric DFT-based methods of spectral analysis. These methods do not offer the high resolution of parametric and eigen-based methods. However, they are attractive in that they are computationally less expensive than model-based methods and are relatively robust. In Section 9.3, we considered the maximum-entropy and the model-based spectral estimation methods. These methods can extrapolate the correlation values beyond the range for which data is available, and hence can offer higher resolution and less side-lobes. In Section 9.4, we considered the eigen-based spectral estimation of noisy signals. These methods decompose the eigen variables of the noisy signal into a signal subspace and a noise subspace. The orthogonality of the signal and noise subspaces is used to estimate the signal and noise parameters. In the next chapter, we use DFT-based spectral estimation for restoration of signals observed in noise.

Bibliography

- BARTLETT M.S. (1950) Periodogram Analysis and Continuous Spectra. *Biometrika*. **37**, pp. 1–16.
- BLACKMAN R.B. and TUKEY J.W. (1958) *The Measurement of Power Spectra from the Point of View of Communication Engineering*. Dover Publications, New York.
- BRACEWELL R.N. (1965) *The Fourier Transform and Its Applications*. McGraw-Hill, New York.

- BRAULT J.W. and WHITE O.R. (1971) The Analysis And Restoration Of Astronomical Data Via The Fast Fourier Transform. *Astron. & Astrophys.* **13**, pp. 169–189.
- BRIGHAM E. , (1988), *The Fast Fourier Transform And Its Applications*. Englewood Cliffs, Prentice-Hall, NJ.
- BURG J.P. (1975) *Maximum Entropy Spectral Analysis*. PhD Thesis, Department of Geophysics, Stanford University, California.
- CADZOW J.A. (1979) ARMA Spectral Estimation: An Efficient Closed-form Procedure. *Proc. RADC Spectrum estimation Workshop*, pp. 81–97.
- CAPON J. (1969) High Resolution Frequency-Wavenumber Spectrum Analysis. *Proc. IEEE*. **57**, pp. 1408–1419.
- CHILDERS D.G., Editor (1978) *Modern Spectrum Analysis*. IEEE Press.
- COHEN L. (1989) Time-Frequency Distributions - A review. *Proc. IEEE*, **77**, pp. 941-981.
- COOLEY J.W. and TUKEY J.W. (1965) An Algorithm For The Machine Calculation Of Complex Fourier Series. *Mathematics of Computation*, **19**, **90**, pp. 297–301.
- FOURIER J.B.J. (1878) *Théorie Analytique de la Chaleur*, Trans. Alexander Freeman; Repr. Dover Publications, 1955.
- GRATTAM-GUINNESS I. (1972) *Joseph Fourier (1768-1830): A Survey of His Life and Work*. MIT Press.
- HAYKIN S. (1985) *Array Signal Processing*. Prentice-Hall, NJ.
- JENKINS G.M. and WATTS D.G. (1968) *Spectral Analysis and Its Applications*. Holden-Day, San Francisco, California.
- KAY S.M. and MARPLE S.L. (1981) *Spectrum Analysis: A Modern Perspective*. *Proc. IEEE*, **69**, pp. 1380-1419.
- KAY S.M. (1988) *Modern Spectral Estimation: Theory and Application*. Prentice Hall-Englewood Cliffs, NJ.
- LACOSS R.T. (1971) *Data Adaptive Spectral Analysis Methods*. *Geophysics*, **36**, pp. 661-675.
- MARPLE S.L. (1987) *Digital Spectral Analysis with Applications*. Prentice Hall-Englewood Cliffs, NJ.
- PARZEN E. (1957) On Consistent Estimates of the Spectrum of a Stationary Time series. *Am. Math. Stat.*, **28**, pp. 329-349.
- PISARENKO V.F. (1973) The Retrieval of Harmonics from a Covariance Function. *Geophy. J. R. Astron. Soc.*, **33**, pp. 347-366
- ROY R.H. (1987) *ESPRIT-Estimation of Signal Parameters via Rotational Invariance Techniques*. PhD Thesis, Stanford University, California.
- SCHMIDT R.O. (1981) *A signal Subspace Approach to Multiple Emitter Location and Spectral Estimation*. PhD Thesis, Stanford University, California.

- STANISLAV B.K., Editor (1986) *Modern Spectrum Analysis*. IEEE Press.
- STRAND O.N. (1977) Multichannel Complex Maximum Entropy (AutoRegressive) Spectral Analysis. *IEEE Trans. on Automatic Control*, **22(4)**, pp. 634–640.
- VAN DEN BOS A. (1971) Alternative Interpretation of Maximum Entropy Spectral Analysis. *IEEE Trans. Infor. Tech.*, **IT-17**, pp. 92–99.
- WELCH P.D. (1967) The Use of Fast Fourier Transform for the Estimation of Power Spectra: A Method Based on Time Averaging over Short Modified Periodograms. *IEEE Trans. Audio and Electroacoustics*, **AU-15**, pp. 70–79.
- WILKINSON J.H. (1965) *The Algebraic Eigenvalue Problem*. Oxford University Press.